A Procedure for Altitude Optimization of Parabolic Nozzle Contours Considering Thrust, Weight and Size

W.B.A. van Meerbeeck
Master Student Aerospace Engineering
Delft University of Technology, Delft, the Netherlands

B.T.C. Zandbergen
Faculty of Aerospace Engineering
Delft University of Technology, Delft, the Netherlands

L.J. Souverein
Space Transportation System Analysis & Modelling
EADS Astrium GmbH, Ottobrunn, Germany

(Dated: December 23, 2012)

The main difference between vacuum and altitude optimization of rocket nozzles is the presence of a performance loss due to the ambient pressure, resulting in an optimum performance nozzle contour with a finite expansion ratio. Using the design of the nozzle of an MMH-NTO engine for sea-level operation, a graphical technique is proposed to optimize a nozzle contour for highest thrust at a certain weight or length. It is found that the contour designed with this technique is very close to the truncated global optimum contour. Compared to a design method for altitude-optimized nozzles which is based on finding the highest thrust contour for a fixed length ratio between 0.70 and 0.85, an increase in thrust of 0.5-1% can be reached at equal nozzle length or weight, depending on mixture ratio, chamber pressure and altitude. The results are obtained using a large parameter study with TDK, and a comparison with CFD simulations is made.

I. NOMENCLATURE

Symbols

A	Area	$[m^2]$
C_F	Thrust coefficient	$[-]$
F	Thrust	$[N]$
KL	Length ratio	$[-]$
L	Length	$[m]$
L'	Normalized Length	$[-]$
p_c	Chamber pressure	$[bar]$
R	Radial coordinate	$[m]$
R_t	Throat radius	$[m]$
X	Axial coordinate	$[m]$
Δ	Difference	$[-]$
ϵ	Expansion ratio	$[-]$
η	Efficiency	$[-]$
θ	Wall angle	$[rad]$

Subscripts

alt	Altitude
c	Contour
div	Divergence
fric	Friction
kin	Kinetic
opt	Optimal
sl	Sea-level
tot	Total
v	Vacuum

Abbreviations

BL	Boundary Layer
CFD	Computational Fluid Dynamics
IC	Ideal Contour
CLO	Constant Length Optimization
CWO	Constant Weight Optimization
LRE	Liquid Rocket Engine
MABL	Mass Addition Boundary Layer
MMH	Monomethylhydrazine
MOC	Method of Characteristics
NTO	Nitrogen Tetroxide
ODE	One-Dimensional Equilibrium
ODK	One-Dimensional Kinetics
TDK	Two-Dimensional Kinetics
TIC	Truncated Ideal Contour
TOC	Thrust Optimized Contour
TOP	Thrust Optimized Parabola

II. INTRODUCTION

The goal of a rocket nozzle is to expand the combustion products at the end of the combustion chamber to high velocities by converting the internal and potential energy into kinetic energy. To maximize the performance, rocket nozzles have to be contoured in a certain way such that optimum expansion is achieved. The minimization of rocket nozzle losses is of great practical importance because even fractions of a percent of nozzle thrust can result in a significant gain in payload [1]. This article describes the design procedure of the divergent part of the nozzle contour of an MMH-NTO rocket engine for sea-level operation.

Rocket nozzles are designed in different ways for operation in vacuum or at sea-level. For vacuum nozzles, it holds that the performance increases continuously with increasing expansion ratio ϵ, and the theoretically highest performance is found at an infinite ϵ. The optimization of performance depends hence mainly on size and weight limitations [2].

Because of the ambient pressure in Earth's atmosphere, an additional performance loss is imposed on a nozzle optimized for sea level, or any altitude in general. For a given combustion chamber design and altitude, this performance loss depends solely on the expansion ratio [3]. A finite expansion ratio can be found, which will result in the highest performance at the design altitude.

The current optimization process for nozzles designed to have highest performance at a certain altitude is based on iteratively finding the optimum expansion ratio for a length ratio between 0.70 and 0.85. The length ratio KL is defined as the ratio between the length of the bell nozzle and the length of a 15-deg conical nozzle with equal expansion ratio. The choice of the length ratio is a trade-off between length and performance. Figure 1 shows the variation of nozzle efficiency with length ratio for inviscid flow. At a length ratio of 0.85, a nozzle efficiency of 99% is reached, and only 0.2% of additional performance can be gained by increasing the length ratio to 1.00. For this reason, $KL = 0.85$ is often taken as upper bound.

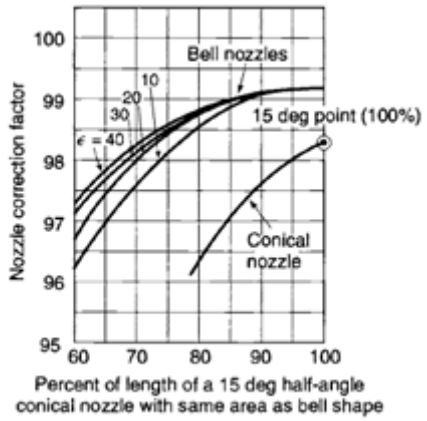

FIG. 1: Variation of bell nozzle efficiency with length ratio and expansion ratio (inviscid flow) [3]

The dimensionless thrust coefficient C_F is used in this study to assess the performance of a nozzle. This makes it easier to compare the nozzle performance of engines with different chamber pressures and mixture ratios. The thrust coefficient is used in many classic papers about nozzle contour optimization, such as [4], [5], [6].

III. NOZZLE TYPES AND LOSSES

Since conical nozzles suffer from high performance losses, practically all current nozzles are bell nozzles. The Ideal Contour (IC) nozzle is constructed using the Method of Characteristics (MOC) and produces a homogeneous flowfield with a constant velocity distribution in the exit area. It offers the highest performance, but is too long and heavy to use in practice. A Truncated Ideal Contour (TIC) nozzle can offer a high weight and length reduction with a relatively small performance loss [6]. The highest performance for a certain length and expansion ratio is however attained with a Thrust Optimized Contour (TOC) nozzle, which can be obtained using the MOC and the calculus of variation as proposed by e.g. Rao [4].

To ease further computations and manufacturing, the TOC can be closely approximated by a skewed parabola (Thrust Optimized Parabola, TOP) with minimum loss of performance [5]. The TOP nozzle can be calculated using Eq. (1), and with normalized coordinates it is entirely defined by four independent variables, i.e. the expansion ratio ϵ, the length ratio KL and the initial and final wall angles θ_i and θ_e, respectively.

$$\left(\frac{R}{R_t} + b\frac{X}{R_t}\right)^2 + c\frac{X}{R_t} + d\frac{R}{R_t} + e = 0 \qquad (1)$$

For vacuum-optimized nozzles, the nozzle losses can be divided into 4 categories.

Kinetic losses: when the combustion products leave the combustion chamber, the reactions are not complete and chemical reactions will continue in the nozzle. The short residence time in the nozzle, coupled with rapidly decreasing pressure and temperature, do not allow the flow to stay in chemical equilibrium, leading to kinetic losses.

Friction losses: losses due to the viscous effects in the boundary layer. This will result in shear stresses and friction losses at the nozzle wall.

Two-dimensional losses: for non-ideal nozzle contours, an inhomogeneous exit flow field is produced due to the two-dimensional expansion. The velocity vectors of the gases exiting the nozzle are not necessarily aligned with the axis of the nozzle or vehicle. As a result, not all of the kinetic energy of the flow results in axial thrust.

Shock losses: losses induced by the internal shock emanating from the throat region of non-ideal nozzle contours. Since both the internal shock losses and the two-dimensional losses depend purely on the expansion of the gasses, they are difficult to calculate separately, and the two losses are generally combined in *divergence losses*.

For altitude optimized nozzles, there is an additional performance loss due to the integral force exerted by the

ambient pressure on the nozzle wall. For inviscid one-dimensional flow, this loss is lowest when the exit pressure equals the ambient pressure.

IV. PARAMETER STUDY PROCEDURE

To find the nozzle contour with highest sea-level C_F for the examined engine, a parameter study is executed to investigate the influence of contour parameters (ϵ, KL and wall curvature) on the nozzle losses.

Only a few studies on the dependencies of nozzle losses on characteristic nozzle design parameters can be found. In Ref. [7], these studies are summarized by Manski and Hagemann: Ref. [8] discusses the friction losses of small N_2H_4 engines with a thrust $F_v = 0.5kN$, whereas Ref. [9] talks about the influence of mixture ratio on the nozzle losses for engines using H_2 and O_2 with $F_v = 4kN$. In their work, Manski and Hagemann investigate the influence of chamber pressure and mixture ratio on the nozzle losses and performance for large $H_2 - O_2$ Liquid Rocket Engines (LRE). Three different expansion ratios and throat radii are examined, whereby KL remains unchanged. No later work was found by the authors with significant new information for the present study.

The previously mentioned papers are focused on vacuum optimization of rocket nozzles. To the best of the authors' knowledge, no parameter studies can be found which focus on the influence of contour parameters on the optimum performance at a certain altitude, apart from ideal rocket theory.

For the design of the nozzle contour of the investigated MMH-NTO engine, a TOP contour was chosen since it is easy to construct, while its performance is close to the maximally achievable TOC performance. The parameter study is performed using the computer program TDK, a commonly used nozzle design tool for LRE in Europe and the United States [10], [11]. TDK is optimized for the simulation of TOP nozzles, allowing a fast and easy variation of contour parameters. The design of the rocket engine till the throat is fixed, and the most important parameters are listed in Table I.

TABLE I: Engine characteristics

Parameter	Value
Fuel	MMH
Oxidizer	NTO
Chamber pressure	38.5 bar
Mixture ratio	1.65

For a given throat radius, the wall contour is only determined by four parameters. Using a direct search method in TDK, the optimal initial and final wall angles can be calculated for a TOP nozzle with fixed expansion ratio and length ratio. This reduces the optimization space from 4 to 2 parameters. An optimization code is written to find the expansion ratio and length ratio for which the highest sea level thrust coefficient is obtained. It was noted that splitting the optimization by separately optimizing the angles did not change the optimum contour parameters.

Due to the modular structure of TDK, shown in Figure 2, the different nozzle losses discussed in the previous section can be calculated. These losses are assessed by their corresponding efficiencies, as shown in Eqs. (2) until (4), where the subscripts denote the thrust coefficient obtained from the particular module, and $\Delta C_{F,BL}$ is the thrust loss in the boundary layer. The calculation of the thrust loss is based on the momentum thickness of the boundary layer, calculated in the MABL module of TDK. The total efficiency η_{tot} is equal to the product of the three different losses, cf. Eq. (5). More information about the working of TDK can be found in [12]. Finite rate kinetics are taken into account in all calculations.

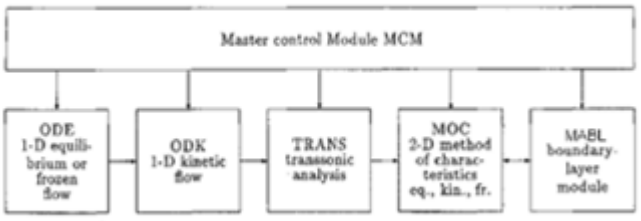

FIG. 2: Modular structure of TDK [12]

$$\eta_{kin} = \frac{C_{F,ODK}}{C_{F,ODE}} \tag{2}$$

$$\eta_{kin} = \frac{C_{F,MOC}}{C_{F,ODK}} \tag{3}$$

$$\eta_{kin} = \frac{C_{F,MOC} - \Delta C_{F,BL}}{C_{F,MOC}} \tag{4}$$

$$\eta_{kin} = \frac{C_{F,MOC} - \Delta C_{F,BL}}{C_{F,ODE}} \tag{5}$$

The optimization code written for the present study consists of two parts: first the optimum expansion ratio is found for different length ratios. This is done using the 'interval halving' optimization method. It is chosen because of its simplicity and relatively fast convergence with a limited amount of simulations [13]. In the interval halving method, exactly one-half of the current interval of uncertainty is deleted in every iteration. It

requires three experiments in the first iteration and two experiments in each subsequent iteration. After the first optimization part is completed, the length ratio of the nozzle with the highest C_F is varied in the same way to find the global optimum. With an initial length ratio step size $\Delta KL = 0.10$, a second iteration loop did not change the global optimum found.

Each simulation consists of 3 steps. In the first step, the optimal wall angles of the inviscid contour are calculated using the built-in function of TDK. In the second step, the boundary layer displacements of this contour are calculated, and a boundary layer correction is applied to the inviscid contour. In the final step, the performance of the new contour is calculated including boundary layer effects.

V. TDK RESULTS

The optimal angles for a large range of expansion ratios and length ratios are given in Figure 3. It is found that a performance increase up to 0.5% can be obtained with respect to a contour where the angles are not optimized.

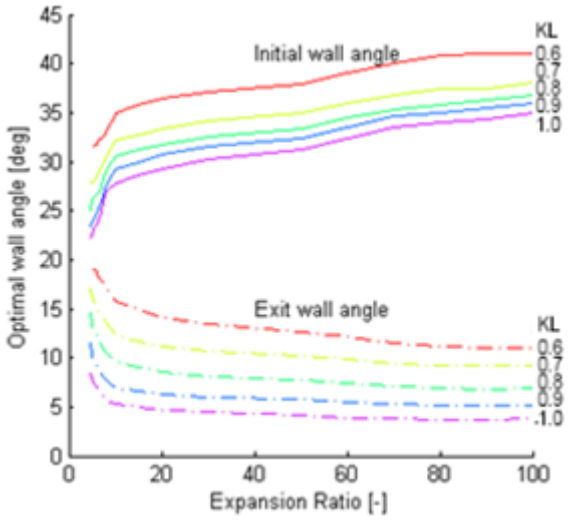

FIG. 3: Variation of θ_i and θ_e with ϵ and KL

Using the optimization code described in the previous section, the performance landscape can be constructed. Figure 4 plots the sea-level thrust coefficient as a function of the contour surface area. This surface area is calculated for the divergent contour. Assuming a constant wall thickness, it provides a good indication of the nozzle weight. Lines of constant ϵ, KL and normalized length $L' = \frac{L}{R_t}$ are visualized in the figure which hence gives a fast overview of the most important influences of geometric parameters on the performance. It can be observed that a significant performance increase ($\succ 1\%$) can still be achieved when comparing the global optimum to the original optimization result for $KL = 0.85$, see Figure 4.

To explain the gain in performance, the sea-level thrust coefficient is plotted as a function of expansion ratio for different length ratios in Figure 5. As can be seen from the figure, a finite optimum expansion ratio can be found for each length ratio. At higher expansion ratios, the performance gain due to higher expansion is cancelled by the increased performance loss due to the ambient pressure. According to the common procedure for altitude-optimized nozzles, i.e. with $KL = 0.85$, a maximum $C_{F,sl}$ of 1.446 can be reached at $\epsilon = 5.617$.

As can be seen from Figure 5, a higher performance can be obtained when the length ratio is increased. Figure 6 shows the variation of nozzle efficiencies for $\epsilon = 10$. Towards low length ratios, a strong decrease in divergence efficiency is observed. In longer nozzles, the flow has more time to become homogeneous, resulting in lower divergence losses. In addition, a longer nozzle will be less heavily curved, resulting in a more parallel flow at the exit. The kinetic efficiency is not significantly influenced by the length ratio. The boundary layer displacement thickness increases with length, resulting in an increase in friction losses. At higher length ratios, the friction losses exceed the decrease in divergence losses. Hence, an optimum length ratio can be found where the combination of all losses is minimized.

From Figures 5 and 7, it can be seen that the optimal length ratio decreases with increasing expansion ratio and vice versa. A global optimum is found at $\epsilon = 5.176$, $KL = 1.26$ with $C_{F,sl} = 1.461$. This is an increase of 1.1% with respect to the optimum found for $KL = 0.85$, however at a length which is 38% larger.

VI. WEIGHT AND LENGTH OPTIMIZED CONTOURS

The global optimum for the investigated engine is relatively long, and consequently heavy. Figure 5 showed that the performance landscape is relatively flat around the global optimum, meaning that contour parameters can be varied significantly, with limited influence on the performance. Combined with the observation that the optimal expansion ratio decreases at higher length ratios, a significant length and weight reduction can be achieved with negligible performance loss by playing on the mutual effect of length ratio and expansion ratio on the performance.

Since weight and dimensions are critical requirements for rocket engines, these parameters also need to be taken into consideration. Figure 4 showed that performance can be gained compared to the optimum obtained using

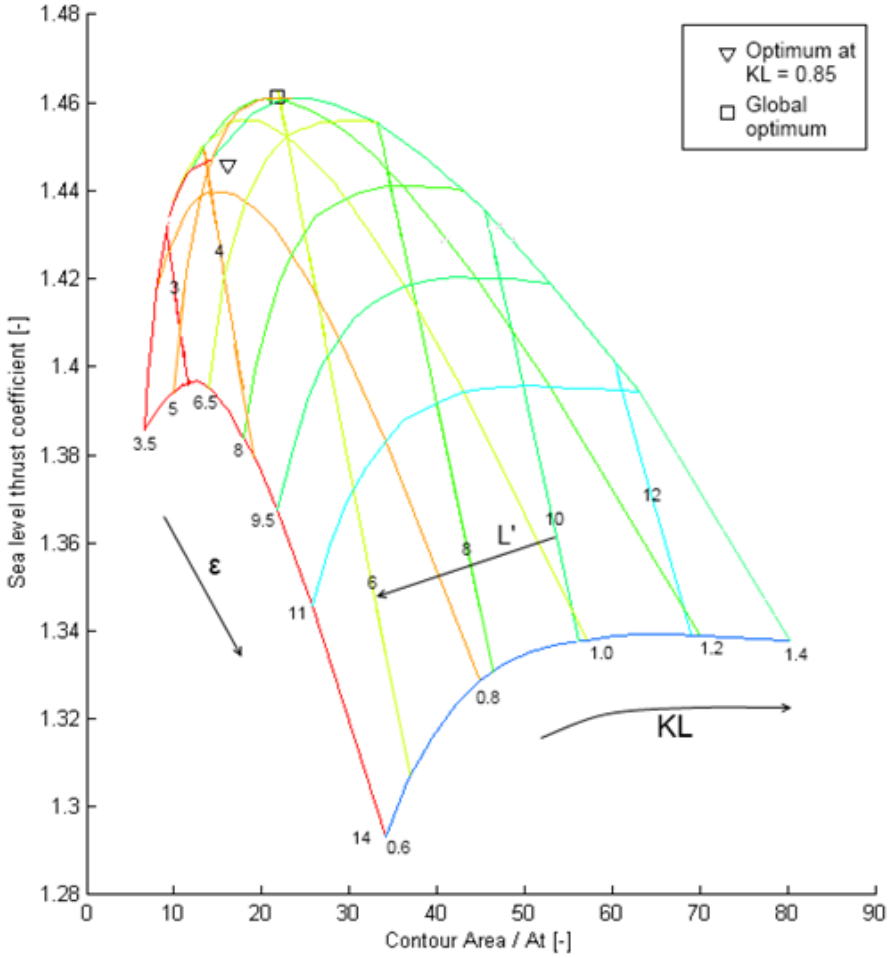

FIG. 4: Performance landscape for sea-level optimization of the MMH-NTO engine

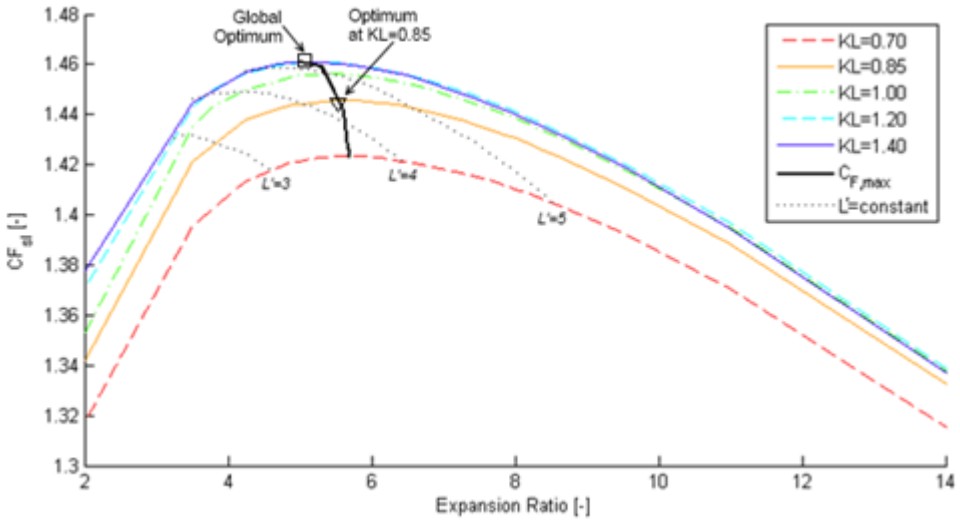

FIG. 5: Variation of $C_{F,sl}$ with expansion ratio for various length ratios

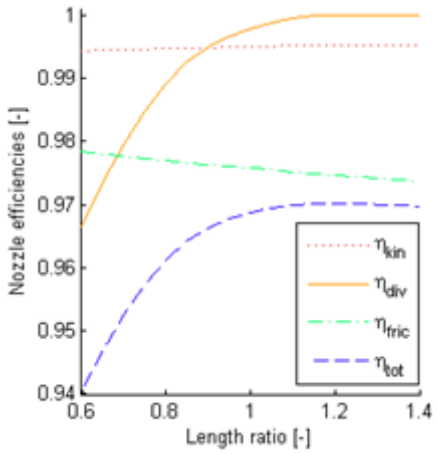

FIG. 6: Variation of vacuum nozzle efficiencies with length ratio ($\epsilon = 10$)

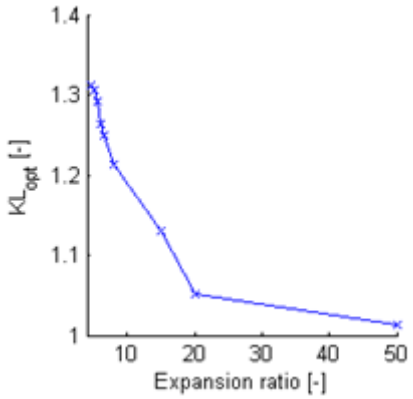

FIG. 7: Variation of optimal length ratio with ϵ

the original method, while keeping the surface area (and hence weight) or nozzle length constant. Figure 8 shows a close-up of the performance landscape normalized by the performance of the global optimum. Using the original procedure, a performance of 98.9% of the maximum performance is reached, but at a 25% lower weight.

Using Figure 8, the contour parameters can be further optimized. Two ways are proposed, based on decreasing the expansion ratio and increasing the length ratio. Keeping the contour weight constant, a further improvement in $C_{F,sl}$ of 0.75% can be gained (Constant Weight Optimization, CWO), corresponding to moving vertically in the diagram. When the absolute nozzle length on the other hand is fixed, around 0.60% performance can be obtained (Constant Length Optimization, CLO), corresponding to moving parallel to the L'-isolines. The contour parameters for both nozzles are listed in Table II.

Also plotted in Figure 8 is the performance of the contours which are obtained by truncating the global optimum at different lengths. It can be observed that the

TABLE II: Optimized nozzle contour parameters

	Parameter	Value
ϵ	4.60	4.54
KL	1.10	4.03
L'	4.70	4.35
$\frac{A_c}{A_t}$	16.1	15.0
$C_{F,sl}$	1.457	1.455

performance of truncated global optimum contours are always very close to the optimal performance for a certain length or weight. Using this information, the following optimization procedure is proposed to find the highest thrust for sea-level and altitude-optimized rocket nozzle contours with size or weight restrictions:

1. Find the global optimum using an optimization algorithm.

2. Truncate the global optimum at the desired length or weight.

VII. INFLUENCE OF OPERATING CONDITIONS

The previous results were found for one set of engine design parameters. Analyzing the influence of operating conditions (p_c, MR, altitude) provides information about the sensitivity of the optimum contour design parameters with respect to these conditions.

Chamber pressure

Figures 9 and 10 show the influence of the chamber pressure on the nozzle efficiencies and the thrust coefficient, respectively. As discussed in [7], an increase in density due to pressure rise leads to a stronger increase of recombination reactions than that of dissociation reactions. The degree of dissociation in the combustion chamber decreases and non-equilibrium effects in the nozzle are reduced, resulting in an increase of the kinetic efficiency. A higher kinetic efficiency due to higher chamber pressure causes more complete energy transformation, and thus, higher gas velocities at the nozzle exit. But the increased velocity is not homogeneously distributed, resulting in higher divergence losses with increased chamber pressure. The friction losses, on the other hand, decrease with chamber pressure since the boundary-layer displacement and momentum thickness decreases as well because it depends inversely on the Reynolds number, which increases with increasing chamber pressure.

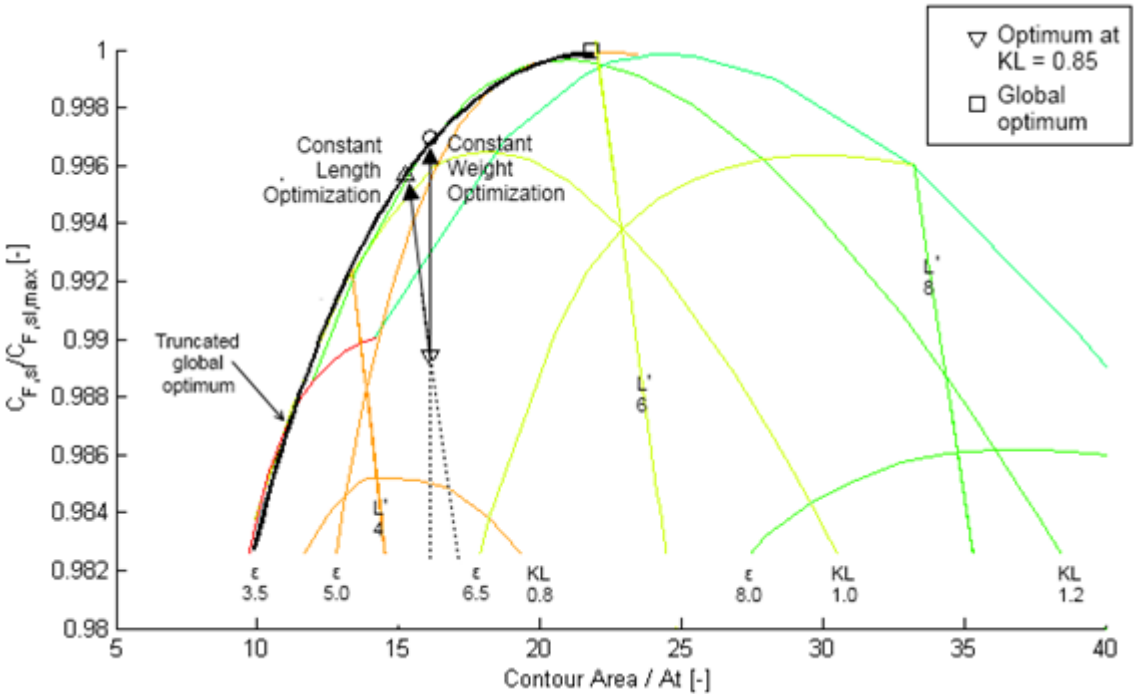

FIG. 8: Close-up of normalized performance landscape

The vacuum performance shows the same trends as the total efficiency in Figure 9, because of the constant nozzle dimensions. The altitude performance will steadily increase, due to the decrease in performance loss caused by the ambient pressure, Eq. (6). However, the optimum contour will change since the increase in chamber pressure causes the nozzle to become underexpanded, as can be seen in Figure 10. Hence, ϵ_{opt} will increase, as does KL_{opt}, although the change in the latter is small (in the order of 1.5% from 20 to 80 bar).

$$C_{F,alt} = C_{F,v} - \frac{p_{alt}}{p_c}\epsilon \tag{6}$$

Since with increasing chamber pressure the influence of the altitude performance loss decreases, the performance landscape around the global optimum is flattened. This means in general that a smaller performance gain can be obtained when optimizing the nozzle contour over a large range of ϵ and KL. On the other hand, with limited performance loss, the possible decrease in length and weight with respect to the global optimum increases significantly with chamber pressure.

Mixture ratio

Figures 11 and 12 show the influence of mixture ratio on nozzle efficiencies and the performance landscape, respectively. Trends in nozzle efficiencies are more difficult to explain because of the different effects of changing mixture ratio on the characteristic velocity and the specific heat ratio. Due to the higher degree of dissociation in the combustion chamber, the kinetic efficiency will decrease when the mixture ratio reaches the stoichiometric value, a trend also discussed in [7]. For MMH-NTO at 38.5 bar, the stoichiometric value is around 2.5. For the same reason, the divergence efficiency will increase. Closer to the stoichiometric value the wall temperatures increase, which will result in higher viscosities, and hence an increased friction in the boundary layer. Therefore, the friction efficiency decreases with values closer to the stoichiometric value.

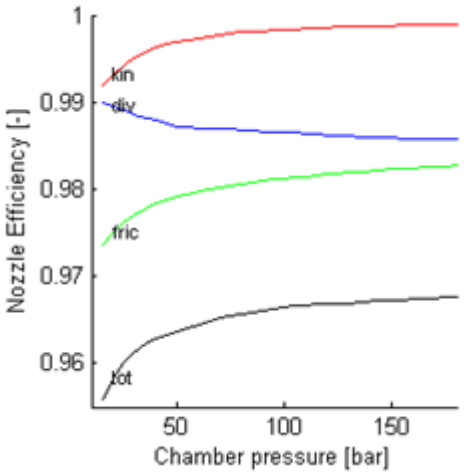

FIG. 9: Inlfuence of chamber pressure on nozzle efficiencies ($KL = 0.85$, $\epsilon = 5.617$, MR=1.65)

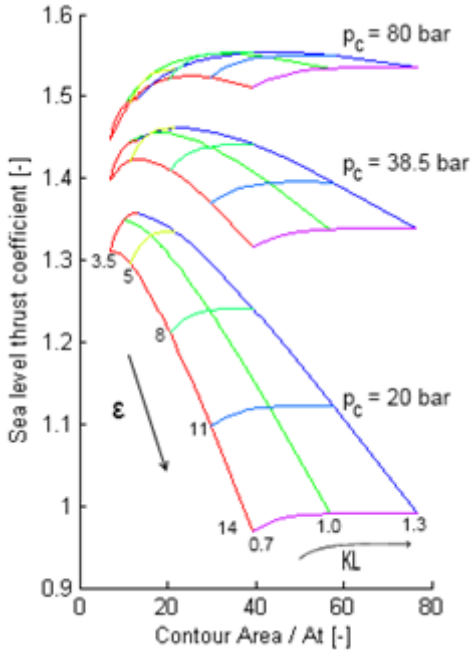

FIG. 10: Influence of chamber pressure on performance landscape (MR=1.65)

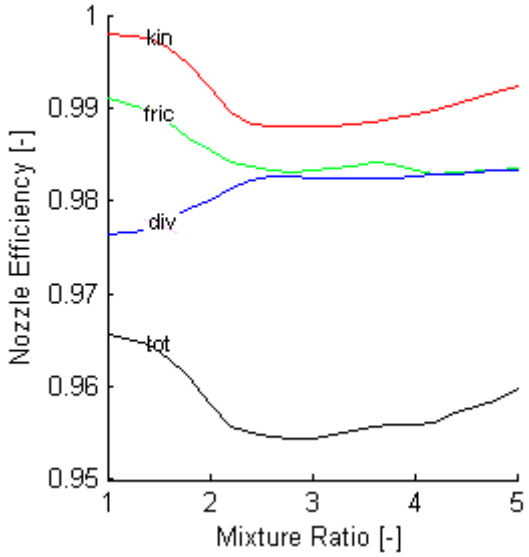

FIG. 11: Inlfuence of mixture ratio on nozzle efficiencies ($KL = 0.85$, $\epsilon = 5.617$, $p_c = 38.5$ bar)

Altitude

Figure 13 plots the influence of the altitude on the performance landscape. The ambient pressure decreases with altitude, which will result in a higher thrust coefficient according to Eq. (6). The effect is therefore similar to an increase in chamber pressure. Since the performance loss depends only on ϵ, the absolute gain

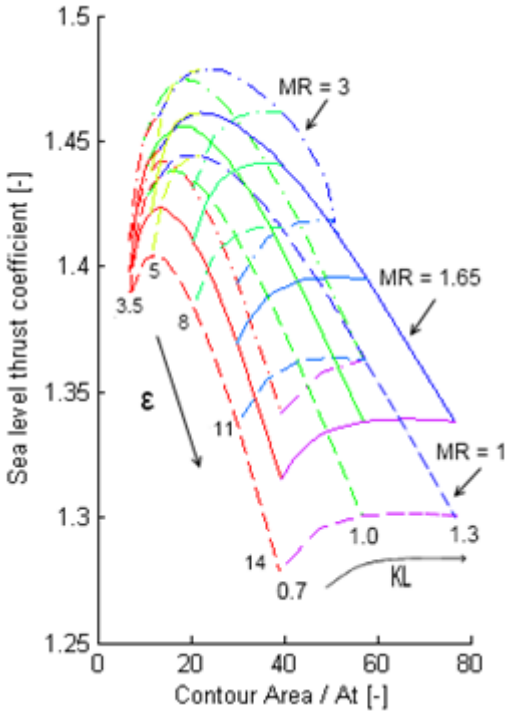

FIG. 12: Inlfuence of mixture ratio on performance landscape ($p_c = 38.5$ bar)

in performance with KL does not change. The same optimal length ratio will be found, but the relative performance gain decreases with increasing altitude. Similar to the effect of chamber pressure, the possible decrease in length and weight with respect to the global optimum increases with altitude for a fixed allowable performance loss.

VIII. VALIDATION WITH CFD

TDK makes use of the method of characteristics to calculate the performance of nozzles. A boundary layer correction is added afterwards. Particularly at higher length ratios, the influence of the boundary layer increases. Because of the flat region in the performance landscape around the global optimum with respect to C_F, these approximations could influence the optimum contour. Therefore, the results obtained with TDK are compared to results obtained using a Navier-Stokes solver, obtaining an independent cross-check for the optimum found with TDK using a different flow solver. The program ANSYS CFX is used for this purpose. To limit the computation time, frozen flow is assumed in the nozzle. The results obtained with CFX are compared to frozen flow results of TDK in Figure 14.

At $KL = 0.85$, the results from CFX match those from TDK. At higher length ratios, a difference is found,

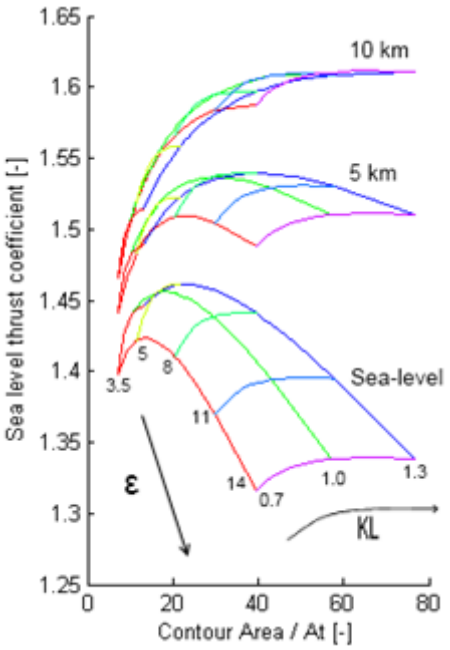

FIG. 13: Inlfuence of altitude on performance landscape (p_c = 38.5 bar, $MR = 1.65$)

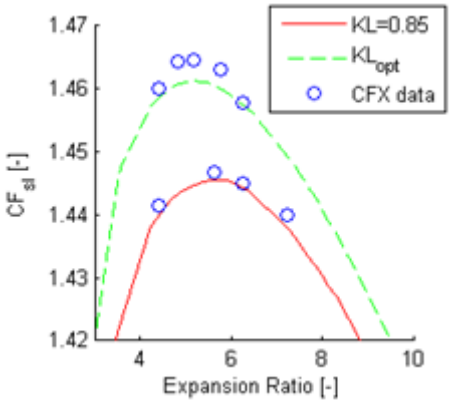

FIG. 14: Comparison of TDK and CFX frozen flow performance data

although it is less than 0.25%. This difference does not affect the optimum expansion ratio, since for both $KL = 0.85$ and $KL = KL_{opt}$, the same optimum is found. This confirms that the optimum contour found using the TDK based approach is flow solver independent and does hence not depend on modelling approaches particular to TDK.

IX. CONCLUSIONS AND RECOMMENDATIONS

Due to the performance loss caused by the ambient pressure, a global optimum contour can be found for any altitude. An optimization procedure is proposed which graphically shows the dependency of the thrust coefficient on weight, nozzle length and expansion ratio. Using this procedure, a nozzle can be constructed which has the highest thrust for a given length and weight, by simply truncating the global optimum contour. Using this method, a performance increase of 0.75% was achieved with respect to the original optimization procedure with KL=0.85 when the weight was kept constant, and an increase of 0.60% with constant length. The possible performance gain depends on the chamber pressure and the altitude, and to a lesser extent on the mixture ratio.

Future research could be focused on a further quantification of the performance gain as a function of the various operating conditions. The effect of shifting the contours towards higher length ratios and smaller expansion ratios could also be investigated for vacuum optimized nozzles. Lastly, since this research was performed for TOP nozzles, a similar study could be started to find out whether the same performance landscape can be found for TOC and TIC nozzles, which are more difficult and time-consuming to construct. If this would be the case, the design process of these nozzles could be simplified by first finding the performance landscape for a TOP nozzles, and converting the final nozzle design to a TOC or TIC contour.

Acknowledgments

This research was performed as part of the master thesis at Delft University of Technology, in cooperation with EADS Astrium Ottobrunn. The authors would like to thank the colleagues at the Space Transportation department of EADS Astrium Ottobrunn for their help and advice.

[1] Sternin, L.E., 'Analysis of the Thrust Characteristics of Jet Nozzles Designed by Various Methods', *Fluid Dynamics* , Vol. 35., No. 1, pp. 123-131, 2000.

[2] Vuillermoz, P., Weiland, C. and Hagemann, G., 'Nozzle Design and Optimization', *Liquid Rocket Thrust Chambers: Aspects of Modeling, Analysis and Design* , Chapter 13, pp. 469-492, American Institute of Aeronautics and Astronautics, 2004.

[3] Sutton, G.P. and Biblarz, O., *Rocket Propulsion Elements*,Wiley, John & Sons, 7 edition, 2001.

[4] Rao, G.V.R., 'Exhaust nozzle contour for optimum thrust' *Jet Propulsion* , vol. 28, pp. 377-382, 1958.

[5] Rao, G.V.R., 'Approximation of optimum thrust nozzle contour', *ARS Journal* , vol. 30, p. 561, 1960.

[6] Ahlberg J.H., Hamilton, S., ea, 'Truncated perfect nozzles in optimum nozzle design'. *ARS Journal* , vol. 31, pp. 614-620, 1961.

[7] Manski, D. and Hagemann, G., 'Influence of Rocket Design Parameters on Engine Nozzle Efficiencies', *Journal of Propulsion and Power* , vol.12, pp. 41-47, 1996.

[8] Buschuite, W., and Hartung, W., 'Der Einfluss der Grenzschicht auf den Schub von Kleinsttriebwerken bei hoher Expansion', *DLRFB-64-48*, Lampoldshausen, Germany, 1964.

[9] Miyajima, H., and Nakahashi, K., 'Low-Thrust Engine Performance with a 300:1 Nozzle',*AIAA Paper 83-1313*, 1983.

[10] Software and Inc. Engineering Associates, 'TDK08', `http://seainc.com/?products=132`, 2012.

[11] Coats, D.E., 'Assessment of Thrust Chamber Performance', *Liquid Rocket Thrust Chambers: Aspects of Modelling, Analysis and Design* , Chapter 17, pp. 601-620. American Institute of Aeronautics and Astronautics, 2004.

[12] Dunn, S.S., and Coats, D.E., 'Two-Dimensional Kinetics nozzle performance computer program', *Software and Engineering Associates, Inc.* , 1991.

[13] Rao, S.S., *Engineering Optimization: Theory and Practice* , Wiley, John & Sons, 2009.